Metabolic Profiling Reveals the Protective Effect of Diammonium Glycyrrhizinate on Acute Hepatic Injury Induced by Carbon Tetrachloride

By: Xiaoyan Wang, Jingchao Lin, Tianlu Chen, Mingmei Zhou, Mingming Su, and Wei Jia

Abstract:

Diammonium glycyrrhizinate (DG), a constituent of Glycyrrhiza uralensis, has a protective effect on hepatic injury, hepatisis and cirrhosis. To date, the mechanism has been poorly understood, especially at the metabolic level. A metabolomic profiling study was performed to characterize the carbon tetrachloride (CCl_4) induced global metabolic alteration and the protective effects of DG in Sprague-Dawley rats. Urinary and hepatic tissue metabolic profiling revealed that CCl_4 perturbed the amino acid metabolism (alanine, glycine, leucine), tricarboxylic acid cycle (citrate), lipid metabolism (unsaturated fatty acids) and gut microbiota related metabolites. Our results also indicated that DG was able to attenuate CCl_4 perturbed metabolic pathways and ameliorated biochemical markers of alanine aminotransferase (ALT), aspartate aminotransferase (AST), and Total cholesterol (TCHO). This global metabolomic approach also revealed full metabolic recovery takes longer than apparent and conventional histological and biochemical markers.

Article:

INTRODUCTION

Diammonium glycyrrhizinate (DG), a purified effective constituent of the traditional Chinese medicinal herb Glycyrrhiza uralensis (liquorices or Gan-Cao) is clinically used in the treatment of hepatic injury, hepatisis and cirrhosis (Feng et al. 2007). DG possesses a high anti-inflammatory effect, which protects the hepatic cell membrane, and ameliorates liver function (Xu et al. 2009; Yuan et al. 2006). It would undoubtedly be beneficial to understand the mechanisms of the hepatoprotective effect of this herbal ingredient in metabolic regulation. Carbon tetrachloride (CCl_4) is a widely used hepatotropic poison which induces experimental liver damage histologically as hepatic steatosis, cellular necrosis, fibrosis, hepatocellular death and carcinogenicity (Weber et al. 2003). Because the CCl_4 induced hepatic injury model can clearly reflect the function, metabolism and morphological variations of hepatic cells with high reproducibility, the model is commonly used to simulate acute/chronic hepatitis (Okamoto and Okabe 2000; Cherkashina and Petrenko 2006) and hepatic fibrosis (Abdel-Salam et al. 2007). The metabolic impact of CCl_4 has been evaluated by profiling differential expressed metabolites of plasma, tissue and urine during poisoning process (Robertson et al. 2000; Pan et al. 2010; Lin

et al. 2009). In this study, we set up an acute hepatic injury animal model with CCl_4 to test the biochemical and metabolic mechanism of the anti-hepatotoxicity of DG.

Metabolic profiling of biological samples using GC/MS has been extensively used to evaluate the toxic/disease status and test the efficacy of drug treatment (Pan et al. 2010; Qiu et al. 2007; Wang et al. 2007). This technology provides quantitative information on metabolite levels increase or decrease in response to xenobiotic interventions, especially in hepatotoxicity research (Chen et al. 2009; Beger et al. 2010; Sun et al. 2009). This information complements organ-specific biochemical and histological variations and can reveal a complex interplay among biochemical regulatory pathways and xenobiotics agents in a given biological system. This study aimed to characterize metabolic variations and thus, understand the dynamic pathophysiological process associated with the CCl_4 induced acute hepatic toxicity and the protective effect of DG pre-ingestion in Sprague-Dawley (SD) rats upon treatment of a diammonium glycyrrhizinate intervention.

MATERIALS AND METHODS

Animals and treatments

A total of 72 Male Sprague-Dawley (SD) rats weighing 200–250 g were commercially obtained from Shanghai Laboratory Animal Co., Ltd. (SLAC, Shanghai, China). All animals were kept in a barrier system with regulated temperature (23–24°C) and humidity (60 ± 10%) and on a 12/12-h light–dark cycle with lights on at 08:00 a.m. The rats were fed certified standard rat chow and tap water ad libitum for 2 week acclimation. Rats were randomly divided into three groups of 24: (A) normal control (NC), (B) CCl_4 model (CCl_4), (C) DG + CCl_4 (DG/CCl_4). Each animal in the DG/CCl_4 group was intragastrically administered 46.88 mg kg^{-1} of DG (dissolved in saline), while rats in the NC and CCl_4 groups received the same volume of saline, once a day for 14 days. On the 14th day, each animal in the CCl_4 and DG/CCl_4 group received an intraperitoneal injection of CCl_4 in olive oil (25% v/v) at 1.5 ml kg^{-1} to induce the acute injury model. Normal control rats received the same volume of olive oil. Eight rats in each group were randomly killed at 24 and 96 h after CCl_4 administration and at the end of the study. The right lobes of the livers (0.5 g) were fixed in a 10% formaldehyde solution, embedded in paraffin and then processed for light microscopy. Another part of each liver was washed with saline, wiped dry, and then homogenized to 10% homogenate with cold saline for further biochemical measurement and metabolic profiling analysis.

Twenty-four hour urine samples of each animal were collected from individually housed rats in metabolism cages at the initial day (I1), the 7th day (I7), and the 1st day (P1), the 4th day (P4), the 7th day (P7) and the 10th day (P10) post CCl_4 administration (Table 1). At the end of the study, after the last time point (P10), urine samples were collected, all the rats were sacrificed and the serum and livers were collected for biochemical measurement. The urine samples were centrifuged at 10,000 rpm for 10 min to remove suspended debris and stored at −80°C. The animal experiment was carried out under the Guidelines for Animal Experiment of Shanghai University of Traditional Chinese Medicine (Shanghai, China), and the protocol was approved by the Animal Ethics Committee of the Shanghai University of Traditional Chinese Medicine.

Table 1: Experimental design and sampling schedule

Time (day)	Abbreviations	Experiment content	Sampling
1	I1	Initial time (pretreatment of DG)	Urine
7	I7	Initial time (pretreatment of DG)	Urine
14		CCl_4 toxication	
15	P1	Post-toxication	Urine, liver tissue, serum
18	P4	Post-toxication	Urine, liver tissue, serum
21	P7	Post-toxication	Urine
24	P10	Endpoint	Urine, liver tissue, serum

Biochemistry and histopathology study

Blood was collected at the 1st (P1), 4th (P4) day after CCl_4 administration and at the end of the experiment (P10). Serum samples were then removed from the coagulated blood after centrifugation ($10,000 \times g$, 10 min, 4°C) and biochemical analysis was performed. Total cholesterol (TCHO) and serum enzymes, including aspartate aminotransferase (AST) and alanine aminotransferase (ALT), were detected using an automatic biochemical analyzer (BST-370) to evaluate the severity of hepatic injury.

Liver tissue was collected at the 1st (P1), 4th (P4) day after CCl_4 administration and at the end of the experiment (P10). The liver malondiadehyde (MDA), superoxide dismutase (SOD) and glutathion peroxidase (GSH-px) content was detected with commercial Malondiadehyde Assay Kit, Superoxide Dismutase, and glutathion peroxidase Assay Kit (Jiancheng Bioengineer Institute, Nanjing, China), respectively. Briefly, liver tissues were homogenized with a T10 basic homogenizer (IKA, Staufen, Germany) for 30 s at 0°C before the procedures were conducted in strict accordance with instruction of the manufacturers. Values of MDA, SOD and GSH-px were obtained from the measurement and the standard curves.

The same part of each liver sample was fixed in 10% (v/v) formalin for at least 12 h, and then processed into wax sections. Tissue sections were subsequently stained with haematoxylin and eosin (H–E), examined under a light microscope (OLYMPUS Co., Ltd, Japan) for the hepatic cell morphology evaluation, and captured by a digital camera.

Data from the serum and tissue biochemistry determination were expressed as mean ± SD. Differences between the means of the treatment and control groups were analyzed using one-way analysis of variance (ANOVA). The critical *P* value was set at 0.05.

Metabolic profiling of urine and hepatic tissue samples

GC/MS-based metabolic profiling was performed on the urine samples following our established methods (Qiu et al. 2007). The urine samples were derivatized with ethylchloroformate (ECF). A 600 μl of diluted urine sample (urine/water) 1:1, v/v) was added with 100 μl of L-2-chlorophenylalanine (0.10 mg/ml, internal standard for batch quality control), 400 μl of anhydrous ethanol, 100 μl of pyridine and derivatized with 50 μl of ECF at room temperature, and then ultrasonicated at 100 kHz for 60 s. The derivatives were extracted with 300 μl of chloroform, and the pH was adjusted with 100 μl of NaOH (7 mol/l). The derivatization process was repeated by adding an additional 50 μl of ECF. The resulting mixtures were centrifuged at 3000 rpm for 3 min. Then, the aqueous layer was removed and the chloroform layer containing derivatives was dehydrated with anhydrous sodium sulfate for subsequent GC/MS analysis. A 1 μl aliquot of the derivatized extract was injected in splitless mode into an Agilent 6890N

GC/5975B inert MSD (Agilent Technologies, Santa Clara, CA, USA). Separation was achieved on a DB-5MS capillary column.

Each 100 mg liver tissue was extracted following the two-step extraction procedure described in our previous report (Pan et al. 2010). Briefly, for each 100-mg liver tissue sample, 500 µl of each of the two solvents (the mixture of chloroform, methanol and water (1:2:1, v/v/v) and methanol alone) were used as the two extraction solvents. After homogenization with the first solvent and centrifugation, a 150-µl aliquot of supernatant was transferred to a separate vial and the deposit was re-homogenized with the second solvent before a second centrifugation. Another 150-µl aliquot of supernatant was drawn out and mixed with the first 150-µl aliquot of supernatant. Then the 300 µl supernatant from the two extraction step was diluted with 300 µl of water. The 600 µl solution was then derivatized with ECF using the aforementioned method.

Either the injection temperature or the interface temperature was set to 260°C; and the ion source temperature was adjusted to 200°C. Initial GC oven temperature was 80°C; 2 min after injection, the GC oven temperature was raised to 140°C with 10°C min^{-1}, to 240°C at a rate of 4°C min^{-1}, to 280°C with 10°C min^{-1} again, and finally held at 280°C for 3 min. Helium was the carrier gas with a flow rate set at 1 ml min^{-1}. The measurements were taken with electron impact ionization (70 eV) in the full scan mode (*m/z* 30–550).

GC-MS Data Analysis

The analysis of GC-MS data was performed with a minor modification to our established methods (Wang et al. 2009). Briefly, unprocessed GC/MS files were converted into NetCDF format via DataBridge (Perkin-Elmer Inc., U.S.A.) and directly processed by our custom scripts in MATLAB (The MathWorks, Inc., U.S.A.). This process performed data smoothing, filtering, de-noising, baseline correction, peak discrimination and alignment (for identification and extraction of the peaks of the chromatogram indicating the existence and intensities of potential metabolites), internal standard exclusion, and normalization to the total sum of the chromatogram (Bao et al. 2009; Wang et al. 2009; Pan et al. 2010). The resulting three-dimensional (retention time, M/Z and Intensity of peaks) matrix was introduced into the SIMCA-P 12.0 Software package (Umetrics, Umeå, Sweden) for multivariate statistical analysis. To ensure the consistency in spectral data transformation and avoid errors introduced to the data processing, we examined the peak areas with relatively high intensities and found no drastic fluctuations among those peaks. The data were mean-centered and then pareto-scaled. The mean-centering procedure subtracts the mean of the data and results in a shift of the data towards the mean. The pareto-scaling technique gives the weight of each variable by the square root of its standard deviation, which amplifies the contribution of lower concentration metabolites but not to such an extent where noise produces a large contribution, this process enhances the identification of metabolites consistently present in the biological samples. The normalized data was analyzed by principal component analysis (PCA) to visualize general clustering, trends, or outliers among the observations. Then, partial least-squares-discriminant analysis (PLS-DA) was conducted to identify the metabolites differentially produced by CCl_4 or DG. R^2X and R^2Y of the model represent the fraction of the variance, while Q^2Y suggests the predictive accuracy of the model. The cumulative values of R^2X, R^2Y and Q^2Y (range of 0 to 1) close to 1 indicate a satisfactory model. To avoid model over-fitting, the PLSDA model was carefully validated by an

iterative 7-round cross-validation with 1/7 of the samples being excluded from the model in each round and random permutation tests (1,000 times).

A VIP parameter (denoting the variable importance) of greater than 1, combined with a correlation coefficient pCorr (indicating the reliability of the loading and VIP value) of ±0.7 was adopted as the cutoff value for selecting the most important variables in terms of the PLSDA model, based on the integrated MS data (Wiklund et al. 2008). Differentially expressed variables were identified by chromatogram-MS data and labeled using thresholds of their fold change and P-values of their Kruskal–Wallis test. In addition to the nonparametric Kruskal–Wallis test, classical one-way analysis of variance (ANOVA) was also carried out to validate the statistical significance of these variables. The critical P value of Kruskal–Wallis and ANOVA was set at 0.05 for this study. Compound identification of metabolites was performed by comparing the mass fragments of the significant variables with those present in commercially available mass spectral databases such as NIST, Wiley, NBS, and the library we established with a similarity threshed of 70%. Finally, about half of them were verified by reference compounds.

RESULTS AND DISCUSSION
Biochemistry and histopathology results
As alanine aminotranferease (ALT) and aspartate aminotransferase (AST) are enzymes located in liver cells that are readily released into the general circulation when liver cells are injured, the two enzymes were measured to monitor the hepatocellular damage. At the 24th hour post CCl_4 administration, the activity of serum ALT and AST increased significantly, while the TCHO level decreased, as shown in Fig. 1. Pretreatment with DG significantly attenuated the alterations of several metabolite levels. At 96 h, the ALT, AST and TCHO activity of every animal in the study recovered to normal status. The value of MDA and SOD in liver changed significantly, and DG was able to attenuate the variation of MDA as well. The activity of GSH-px was altered by CCl_4 and DG, but not significantly. At the end point of the study, hepatic MDA, SOD and GSH-px levels returned to normal.

The liver sections stained with H–E were examined for the histopathological assessment of CCl_4 induced liver injury and DG's protection (Fig. 2). At the first day post injection of CCl_4, significant damage to the hepatic histology structure, including cytoplasmic vacuolization, cell swelling, variations in cellular size and morphology and inflammatory cell infiltrations, was observed in most CCl_4 challenged samples (Fig. 2b), compared with the normal liver morphologies in the NC group (Fig. 2a). Samples from the DG/CCl_4 group illustrate reduced liver damage, e.g. intact liver structure and inconspicuous inflammatory cell infiltration (Fig. 2c). At 96 h post-dose of CCl_4, all the damage was repaired and the histology showed no difference from the normal tissue (Fig. 2d, e). We ruled out the possible therapeutic effect due to the use of olive oil as a vehicle in our short-term (1–4 day) study, since the anti-inflammatory effects were generally observed in the subjects with relatively long-term (several weeks) dietary supplementation with olive oil (Beauchamp et al. 2005).
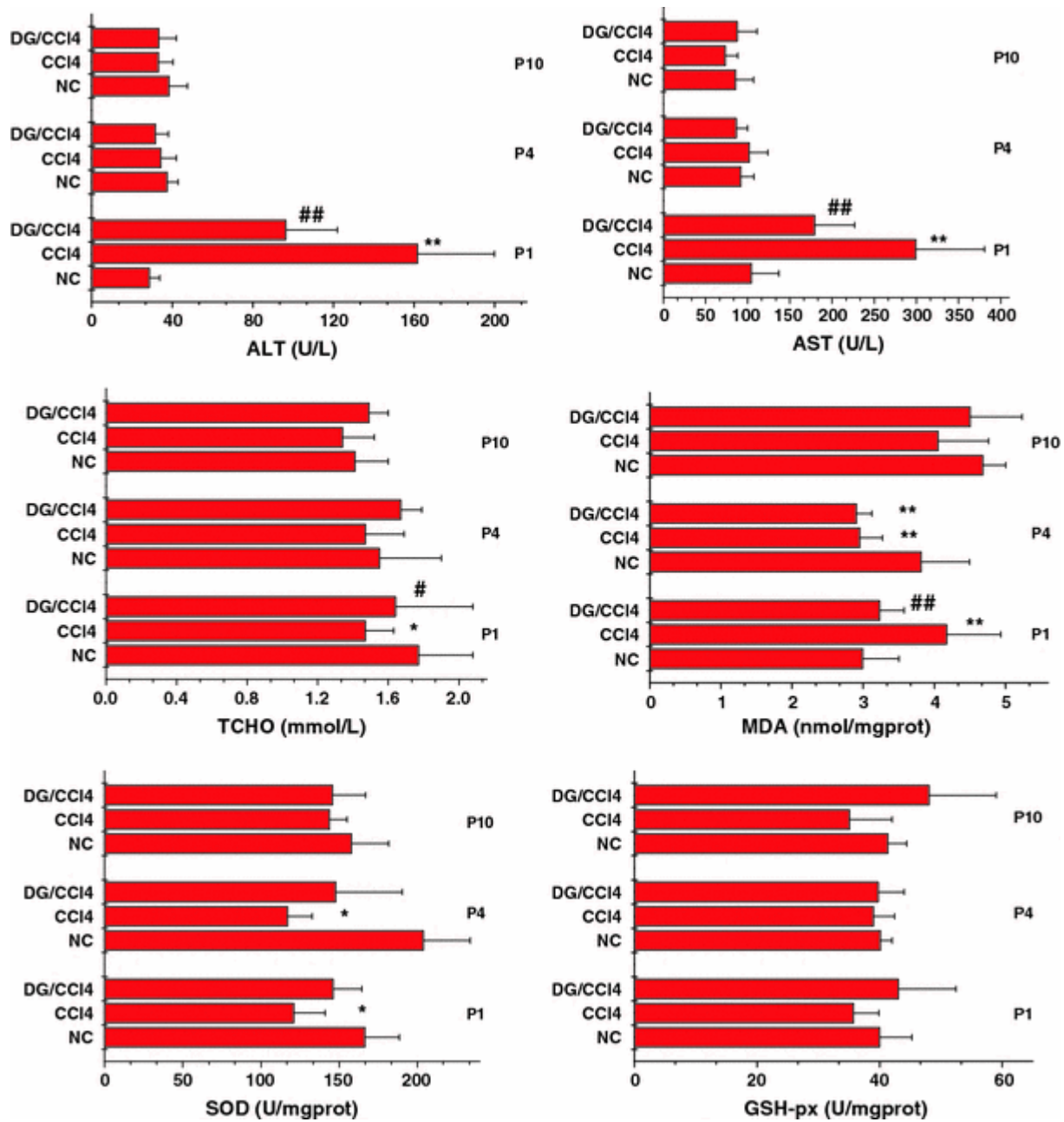
Figure 1: Influence on plasma biochemical activities in rats at the 1,4,10 days after CCl_4 injection ($m \pm s$, $n = 8$). ** $P < 0.01$, * $P < 0.05$ vs. NC ## $P < 0.01$; # $P < 0.05$ vs. CCl_4
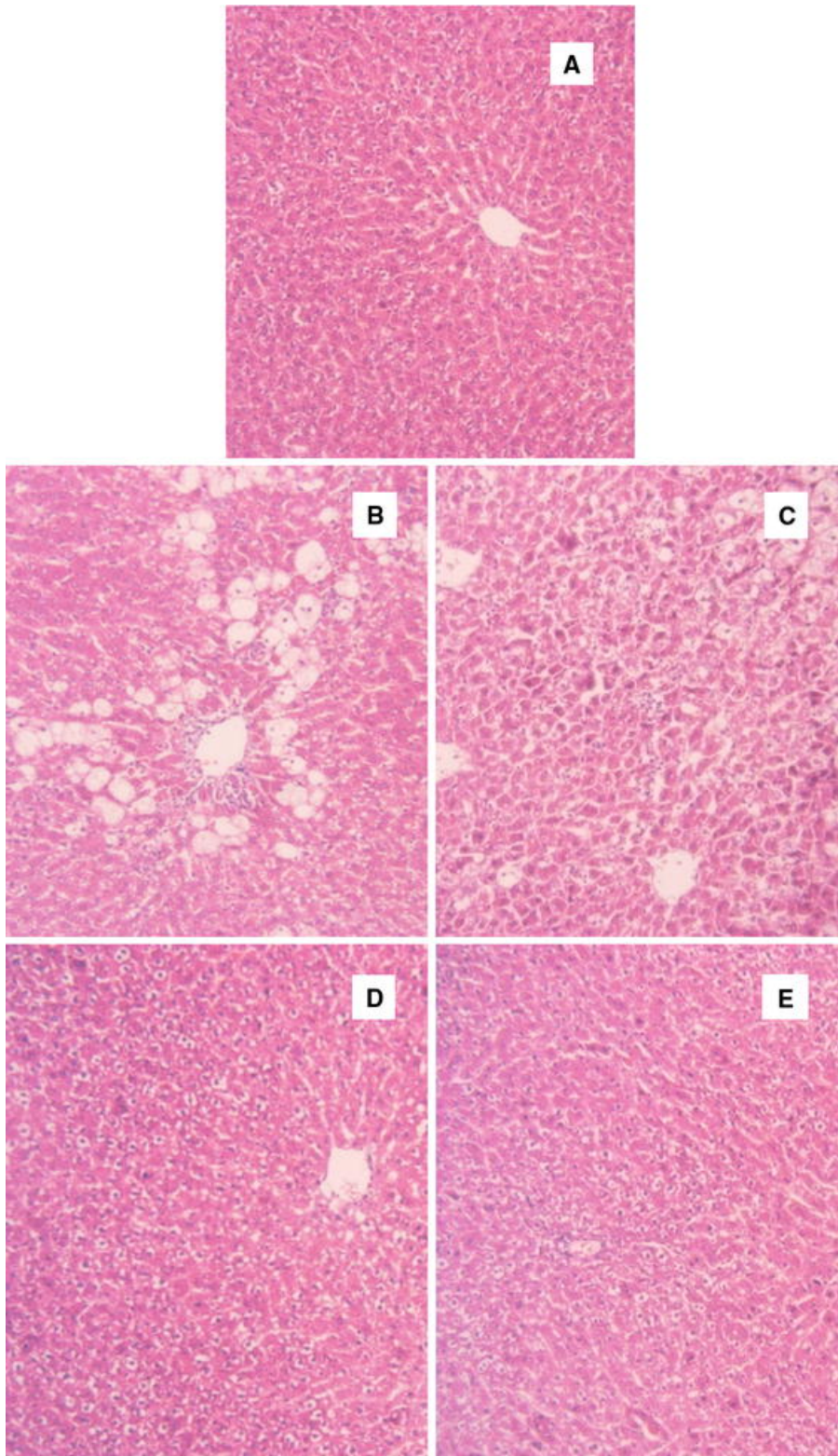
Figure 2: Liver histology (*200) of chemical liver injury's rats induced by CCl_4. **a** NC group; (**b**) the 1st day post dose in CCl_4 group; (**c**): the 1st day post dose in group; (**d**) the 4th day post dose in CCl_4 group; (**e**) the 4th day post dose in DG/CCl_4 group

Metabolite Variation Induced by CCl_4

The PCA scores plot derived from the GC/MS data shows the clustering of NC and CCl_4 groups on the first two principal components (PC1 and PC2), as depicted in Fig. 3a. The metabolomic result of this liver injury model displays stable cumulative modeled variation and good prediction capability with the first two components (Component Number = 3, $R^2Xcum = 0.626$ and $Q^2Ycum = 0.864$). The 3-dimensional scores plot derived from the GC/MS data of the CCl_4, DG/CCl_4 and NC group is depicted in Fig. 3b (Component Number = 3, $R^2Xcum = 0.635, Q^2Ycum = 0.408$).
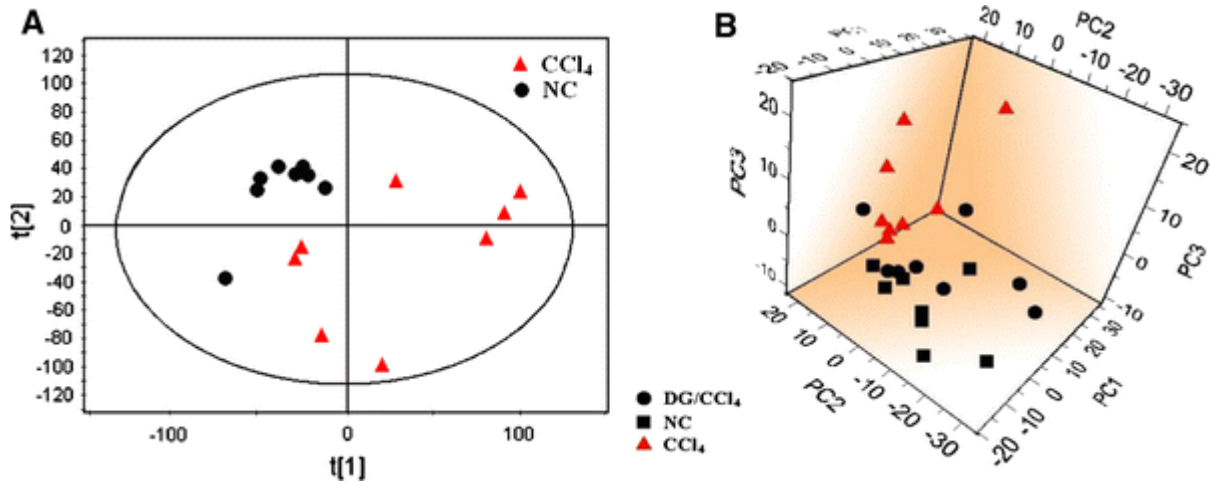
Figure 3: Metabolic profiles depicted by 2D PCA scores plot of GC/MS spectral data from the urine of CCl_4 and NC group (**a**: Component Number = 3, $R^2Xcum = 0.626$ and $Q^2Ycum = 0.864$), and 3D PCA scores plot of GC/MS spectral data from the urine of CCl_4, DG/CCl_4 and NC group (**b**: Component Number = 3, $R^2Xcum = 0.635, Q^2Ycum = 0.408$) 1 day post injection of CCl_4

The trajectories of PCA scores derived from the CCl_4 (Component Number = 2, $R^2Xcum = 0.296, Q^2Ycum = 0.170$) and DG/$CCl_4$ group (Component Number = 2, $R^2Xcum = 0.293, Q^2Ycum = 0.109$) were illustrated in Fig. 4. Transient shifts in the trajectory plot revealed the dynamic progress of the metabolic variation induced by CCl_4 alone or in combination with DG treatment. In the CCl_4 group, the metabolic profile on the first day post-CCl_4 injection (P1) was distinct from those of the other time-points. The trajectory demonstrates that the metabolic regulatory network underwent the most significant metabolic fluctuations on the first day of exposure to CCl_4, and that the perturbed network underwent a recovery process during the following time points, returning to a stable profile close to the pre-dose state. This is consistent with the biochemical markers results. The time-dependent trajectory of metabolic alteration in the DG/CCl_4 group appears similar to that in the CCl_4 group. However, the metabolic perturbation in the DG/CCl_4 group at the 1st and 4th day post-dose of CCl_4 appeared less significant than those in the CCl_4 group.
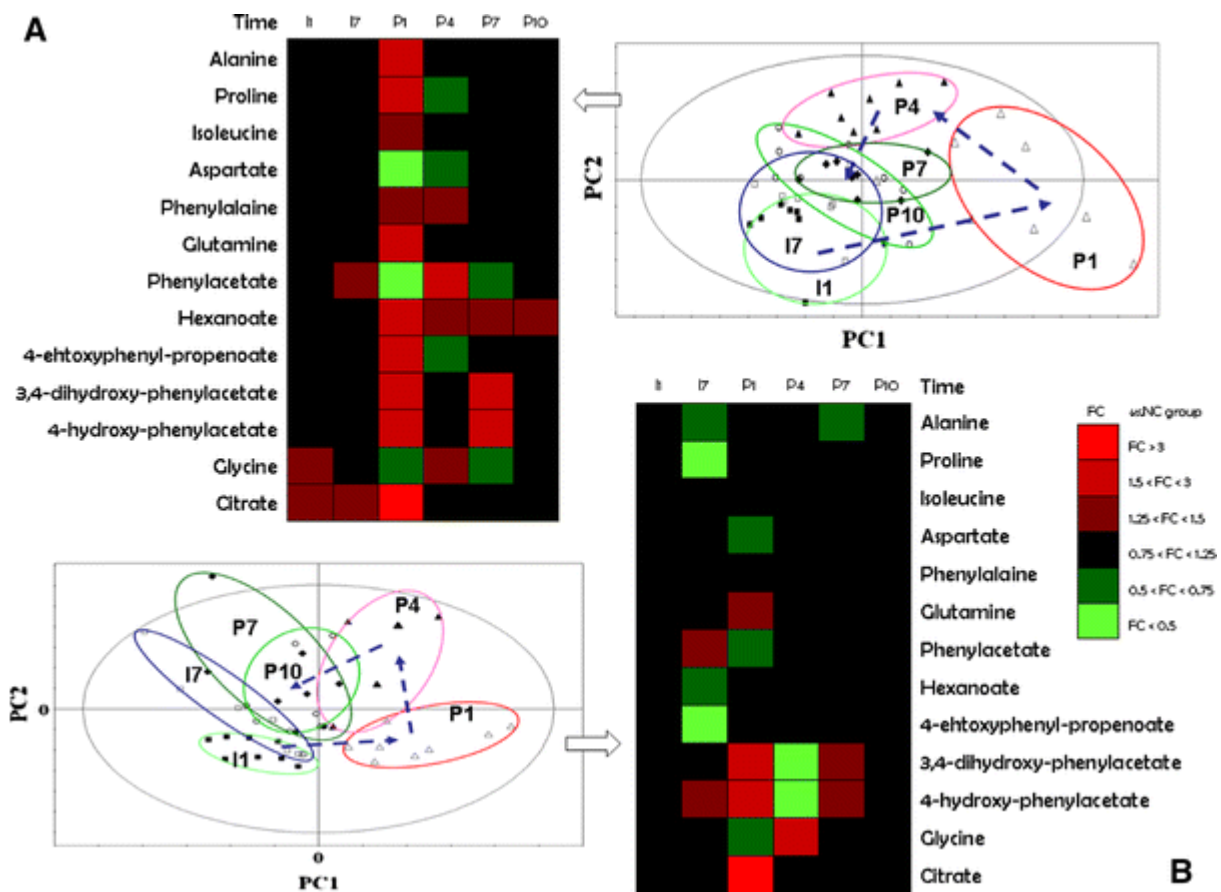
Figure 4: PCA scores plots of GC/MS spectral data from model CCl_4 group (**a**: Component Number = 2, $R^2Xcum = 0.296, Q^2Ycum = 0.170$) and CCl_4/DG group (C) visualized using a metabolic profiling approach, with the heatmap plot of differential expressed metabolites(**b**: Component Number = 2, $R^2Xcum = 0.293, Q^2Ycum = 0.109$) (*filled square* I1, *open square* I7, *open diamond* P1, *filled triangle* P4, *filled diamond* P7, *open circle* P10)

We selected the different expressed metabolites in the rats of CCl_4 group relative to NC group at the 1st day (P1) post CCl_4 exposure, a key time point of liver injury study, and evaluated their variances at different time points of the DG/CCl_4 group (Grizzi et al. 2003). Sixteen out of 21 differentially expressed peaks, including amino acids such as alanine, glycine, proline, and glutamine, and organic acids such as citrate and hexanoate, were identified from spectral dataset, verified by reference standards (Fig. 4; Table 2). Univariate statistical methods, including one-way ANOVA and the nonparametric Kruskal–Wallis test, were utilized to verify the significance of multivariate statistical method. The two heat-maps generated using differentially expressed metabolites in rats also indicate less significant fluctuation of metabolite levels (in fold change, relative to NC) in the DG/CCl_4 group, suggesting that DG could attenuate the metabolic perturbation in the rats exposed to CCl_4. These results support the clinical findings that DG has a protective effect on liver injuries.

Table 2: List of identified differential metabolites in the urine samples of CCl_4 and DG/CCl_4 at 1 day after CCl_4 toxication, P values in CCl_4 and DG/CCl_4

Metabolites	RT[a]	VIP[b]	P [c]	
			CCl_4	DG/CCl_4
Hexanoate[d]	6.06	1.45	0.0306	0.6770
Phenylacetate[d]	7.13	1.19	0.0003	0.0332
Alanine[d]	7.51	1.06	0.0359	0.1750
Glycine[d]	7.62	1.19	0.0049	0.0331
Leucine[d]	10.42	1.52	0.0049	0.0574
Isoleucine[d]	10.70	1.53	0.0427	0.3771
Proline[d]	11.12	1.36	0.0206	0.1937
Unknown	12.84	1.67	0.0382	0.3171
Aspartate[d]	14.03	1.29	0.0026	0.0526
Glutamine[d]	14.42	1.67	0.0004	0.0073
3,4-dihydroxy-phenylacetate[d]	14.87	1.09	0.0419	0.0203
Citrate[d]	15.05	1.21	0.0002	0.0031
Unknown	15.28	1.33	0.0239	0.0552
Unknown	16.01	1.07	0.0298	0.2346
Unknown	17.42	1.02	0.0658	0.2600
Phenylalanine[d]	18.28	1.59	0.0273	0.2207
4-hydroxy-phenylacetate[d]	18.46	1.49	0.0467	0.0574
Indol-3-acetate[d]	21.28	1.19	0.0331	0.0426
Tyramine[d]	26.16	2.07	0.0002	0.0194
4-ehtoxyphenyl-propenoate[d]	29.55	1.69	0.0071	0.1296
Unknown	33.46	1.81	0.0046	0.0172

[a]Retention time of the metabolites in GC/MS
[b]Variable importance in the projection (VIP) was obtained from PLS-DA
[c] P values were calculated from Kruskal–Wallis test *vs.* NC group
[d]Metabolites verified by reference compounds, others were directly obtained from library searching

Significantly expressed metabolites in liver tissues were also analyzed by the Kruskal–Wallis test and classical one-way analysis of variance (ANOVA). *P*-values were set at 0.05. Figure 5 is the heat-map of the fold changes of differentially expressed metabolites in CCl_4 and DG/CCl_4 groups, which consistently shows alleviative effect in DG/CCl_4 group. Decreased levels of alanine, glycine, valine, leucine, arachidonate and eicosapentaenoate, increased levels of aspartate and oleate were observed in CCl_4 group at the 1st (P1) and 4th day (P4). Except for arachidonate, the alteration of these metabolites was attenuated in DG/CCl_4 group at the 4th day. There was no significant variation in the metabolites of liver tissues in the two groups at the last time point.
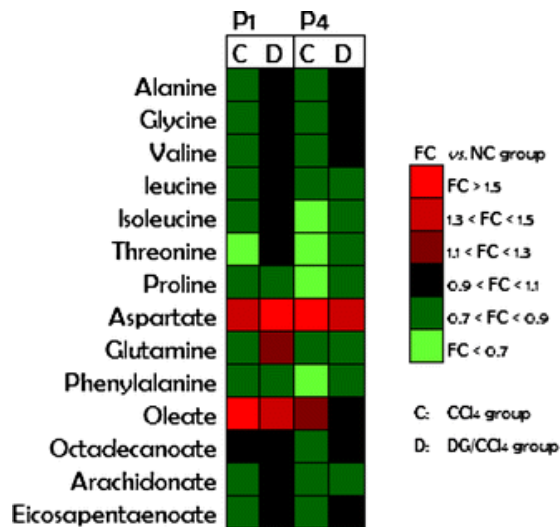
Figure 5: Differential expressed metabolites in liver tissue the 1st and 4th day post intoxication

Potential pathways associated with CCl4 and the DG treatment

Our metabolic profiling strategy of urine and liver tissues is able to reveal the multi-pathway metabolic perturbation associated with CCl_4 and the DG treatment, as summarized in Fig. 6. Since the liver is the hub of amino acids metabolism, any hepatic injury might induce amino acids metabolic disturbances. The metabolomic results showed that most of the amino acids that increased in urine and decreased in liver tissue, such as alanine, proline, glutamine, phenylalanine and isoleucine. Generally, the impact of acute liver injury on amino acids concentration results from three factors: protein synthesis and catabolism, BCAAs (branched chain amino acids) metabolism, and hepatic amino acid clearance. When damage occurs, catabolism promoting hormones, such as glucocorticoids and catecholamines, increase in secretion and decrease in deactivation, resulting in increased protein catabolism and therefore, increased levels of a number of amino acids in systemic circulation. Many amino acids are metabolized by liver enzymes and hence directly associated with the activity of hepatic enzymes. ALT and AST, two important enzymes in liver, were detected as well. Glutamine is an important amino acid for maintaining nitrogen balance (Brosnan 2003). A decrease in liver and an increase in urinary excretion of glutamine may be associated with an outflow of AST from hepatocellular mitochondrion and an indication of impaired hepatic regulating function. Branched chain amino acids (BCAAs), such as valine, isoleucine and leucine, are essential amino acids typically involved in stress, energy and muscle metabolism (Choudry et al. 2006). In our study, an increased level of isoleucine and leucine in urine, while decreased levels of hepatic valine, leucine and isoleucine were observed in CCl_4 group at the 1st and 4th day post CCl_4 injection (P1, P4). When protein catabolism is being observed, as in some cases of severe toxicity, the BCAAs are used in muscle to create alanine, which is then shuttled to the liver (Holecek et al. 1996). Normally blood alanine is transported to liver via glucose-alanine cycle to generate pyruvate which becomes a source of carbon atoms for gluconeogenesis. Alanine was found largely excreted in urine and decreased in liver tissue, suggesting an impaired glucose-alanine cycle due to the CCl_4 exposure. DG attenuated the altered levels of alanine and BCAAs but didn't affect citrate level, suggesting that DG's interaction is involved in the glucose-alanine cycle and its closely associated amino acids metabolism. It was not able to ameliorate the citrate expression level as part of the impaired TCA cycle, whose metabolic enzymes located in mitochondria (Fig. 6).

Aspartic acid is vitally important to the metabolism and construction of many amino acids and intermediates in the tricarboxylic acid (TCA) cycle. It has also shown a protective action on the liver by its capacity to reestablish the cellular deficit of pyridine nucleotides and thus improve the synthesis of nucleic acids, glycoprotein and glycolipids and/or by its participation in various metabolic pathways (Fodor et al. 1976). In this study, aspartate remained a significant higher concentration in the liver at the 1st and 4th day post CCl_4 injection, while its decrease in urine excretion could be resisted by either recovery time or DG treatment.

Urinary and hepatic glycine levels significantly decreased after CCl_4 exposure. The large amounts of oxygen free radicals generated from CCl_4 dose altered hepatic levels of MDA, SOD and GSH-px. As a result, the anti-oxidants involving reduced glutathione hormone (GSH) were presumably over-consumed. As glutathione is synthesized from the amino acids L-cysteine, L-glutamate and glycine, it is understandable that glycine was found significantly depleted soon after CCl_4 exposure. However, we were surprised to detect a drastically increased level of

glycine in urine (Fig. 4a) while decreased in the liver (Fig. 5, P4) 4 days after toxication. Recent research has indicated that glycine significantly decreases liver injury via a direct effect on hepatocytes (Froh et al. 2008). As the decreased hepatic glycine level was normalized by DG at both the 1st and 4th day after injury, we presumed that the elevation of glycine in the urine may be beneficial to the recovery of hepatic cells. The urinary glycine level also displayed a rebound in DG/CCl$_4$ group at P4.
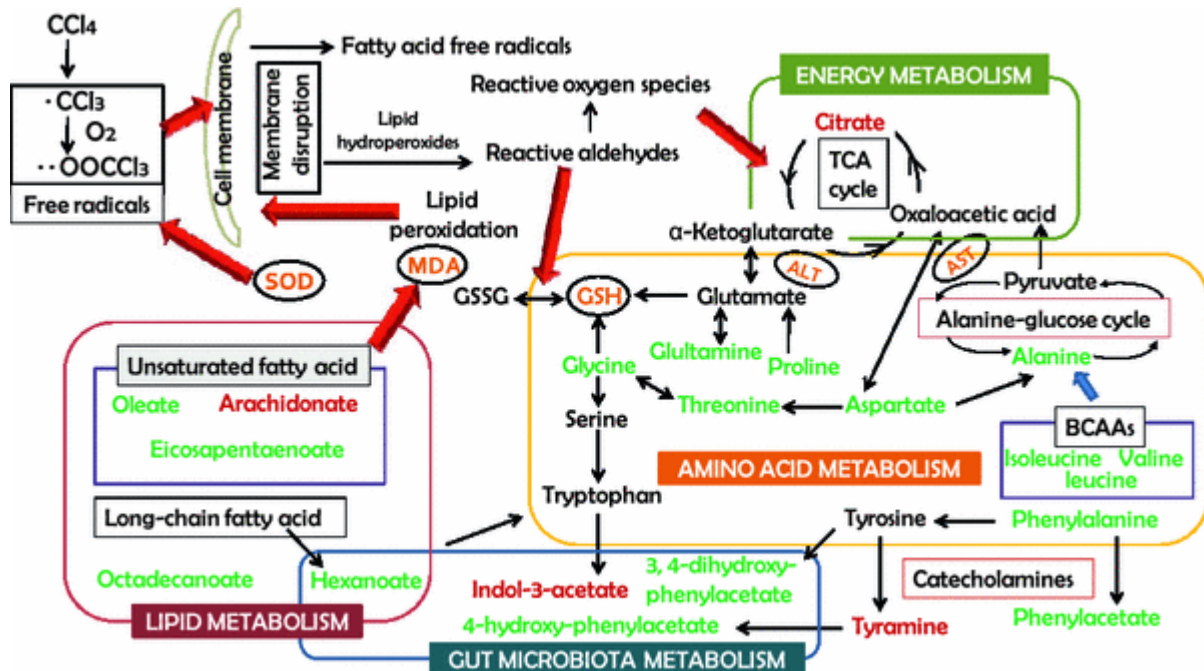
Figure 6: Potential metabolic mechanisms of CCl$_4$ induced toxicity and the protection of Diammonium glycyrrhizinate. All the colored character styles were connected with CCl$_4$ induced toxicity. *Green*: DG effective metabolites; *Red*: DG ineffective metabolites; *Orange*: biochemical indices

Furthermore, several compounds containing benzene ring, such as phenylacetate, phenylalanine, 4-hydroxy-phenylacetate, indol-3-acetate, tyramine, 3, 4-dihydroxy-phenylacetate and 4-ethoxyphenyl-propenoate were discovered significantly altered in the urine of CCl$_4$ treated rats, as compared to the normal group. These metabolites are mainly produced from aromatic compounds, especially aromatic amino acids. Indol-3-acetate, namely indoleacetic acid (IAA) is produced in tryptophan metabolism often with involvement of bacteria in the mammalian gut (Maillet et al. 2009). It is believed to be a product of the decarboxylation of tryptamine or the oxidative deamination of tryptophan. Tyramine is formed by decarboxylation of tyrosine in tissues as well as in the gut (Asatoor 1968). Phenylacetate can be produced by the transamination and then decarboxylation of excess phenylalanine, an important precursor of tyrosine, which decreased in liver and increased in urine at the 1st day post dose. 4-hydroxy-phenylacetate is an oxidative deaminated metabolite of tyramine and also a metabolite of tyrosine from enteric bacteria (Rechner et al. 2004, Nowak and Libudzisz 2006). Another phenolic acid, 3, 4-dihydroxy-phenylacetate, commonly called DOPAC, is the product of oxidation of the aldehyde produced by deamination metabolite from dopamine, one of the catecholamines derived from tyrosine (Goldstein et al. 2003). DOPAC is also one of the major phenolic acids formed during

gut microbial fermentation of diets. The variation of these metabolites may reflect either an alteration in a disturbed symbiotic gut microbiota and/or the catecholamine metabolic pathway. Furthermore, the aromatic metabolites still fluctuated at the P4 and P7, and finally returned to the normal level, suggesting that the impact of CCl_4 on the metabolism of aromatic compounds lasted longer than its impact on other metabolic pathways. The normalized expression level of these metabolites in the DG/CCl_4 group suggests a protective effect of DG on gut microbiota and/or catecholamine pathways.

It has been reported that CCl_4 derived free radicals may attack polyunsaturated fatty acids (PUFA) in cell membranes, forming fatty acid free radicals, which initiate an autocatalytic lipid peroxidation process and generate more lipid hydroperoxides and reactive hydroxyalkenals during membrane disruption (Vulimiri et al. 2010; Catala 2009). The toxin, CCl_4, can also promote the production of fatty acids and triglyceride inside the liver, accelerate the lipid esterification and cholesterols synthesis, and thus, lower the content of partially unsaturated fatty acids (Boll et al. 2001). In our results, octadecanoate, arachidonate and eicosapentaenoate decreased in tissue samples at the 1st or 4th day. We found that the hepatic content of oleate increased at both the 1st and 4th day. DG significantly inhibited the alteration of these fatty acids except arachidonate, suggesting that the anti-inflammatory effect of DG is not directly associated with arachidonate metabolism.

CONCLUDING REMARKS
Our metabolic profiling has revealed the CCl_4 induced alterations in amino acid, TCA, lipid and gut microbiota metabolism. Most of these metabolic alterations could be attenuated by Diammonium glycyrrhizinate. This global metabolomic approach also revealed that the experimental rats required a prolonged recovery in metabolic profile, although the histological results and biochemical markers indicated a rapid recuperation from CCl_4 induced liver injury.

ABBREVIATIONS
DG   Diammonium glycyrrhizinate
NC   Normal control
TCHO   Total cholesterol
AST   Aspartate aminotransferase
ALT   Alanine aminotransferase
MDA   Malondiadehyde
SOD   Superoxide dismutase
GSH-px   Glutathion peroxidase
ECF   Ethylchloroformate
PCA   Principal component analysis
PLS-DA   Partial least squares discriminant analysis

PC   Principal component
GSH   Reduced glutathione
GSSG   Oxidized glutathione
DOPAC   3,4-Dihydroxy-phenylacetate

REFERENCES

Abdel-Salam, O. M., Sleem, A. A., & Morsy, F. A. (2007). Effects of biphenyldimethyl-dicarboxylate administration alone or combined with silymarin in the CCL4 model of liver fibrosis in rats. *ScientificWorldJournal, 7*, 1242–1255.

Asatoor, A. (1968). The origin of urinary tyramine. Formation in tissues and by intestinal microorganisms. *Clinica Chimica Acta, 22*, 223–229.

Bao, Y., Zhao, T., Wang, X., Qiu, Y., Su, M., Jia, W., et al. (2009). Metabonomic variations in the drug-treated type 2 diabetes mellitus patients and healthy volunteers. *Journal of Proteome Research, 8*, 1623–1630.

Beauchamp, G. K., Keast, R. S., Morel, D., Lin, J., Pika, J., Han, Q., et al. (2005). Phytochemistry: ibuprofen-like activity in extra-virgin olive oil. *Nature, 437*, 45–46.

Beger, R. D., Sun, J., & Schnackenberg, L. K. (2010). Metabolomics approaches for discovering biomarkers of drug-induced hepatotoxicity and nephrotoxicity. *Toxicology and Applied Pharmacology, 243*, 154–166.

Boll, M., Weber, L. W., Becker, E., & Stampfl, A. (2001). Pathogenesis of carbon tetrachloride-induced hepatocyte injury bioactivation of CCI4 by cytochrome P450 and effects on lipid homeostasis. *Z Naturforsch C, 56*, 111–121.

Brosnan, J. T. (2003). Interorgan amino acid transport and its regulation. *Journal of Nutrition, 133*, 2068S–2072S.

Catala, A. (2009). Lipid peroxidation of membrane phospholipids generates hydroxy-alkenals and oxidized phospholipids active in physiological and/or pathological conditions. *Chemistry and Physics of Lipids, 157*, 1–11.

Chen, C., Krausz, K. W., Shah, Y. M., Idle, J. R., & Gonzalez, F. J. (2009). Serum metabolomics reveals irreversible inhibition of fatty acid beta-oxidation through the suppression of PPARalpha activation as a contributing mechanism of acetaminophen-induced hepatotoxicity. *Chemical Research in Toxicology, 22*, 699–707.

Cherkashina, D. V., & Petrenko, A. Y. (2006). Hepatoprotective effect of fetal tissue cytosol and its thermostable fraction in rats with carbon tetrachloride-induced hepatitis. *Bulletin of Experimental Biology and Medicine, 141*, 544–547.

Choudry, H. A., PAN, M., Karinch, A. M., & Souba, W. W. (2006). Branched-chain amino acid-enriched nutritional support in surgical and cancer patients. *Journal of Nutrition, 136*, 314S–318S.

Feng, C., Wang, H., Yao, C., Zhang, J., & Tian, Z. (2007). Diammonium glycyrrhizinate, a component of traditional Chinese medicine Gan-Cao, prevents murine T-cell-mediated fulminant hepatitis in IL-10- and IL-6-dependent manners. *International Immunopharmacology, 7*, 1292–1298.

Fodor, O., Schvartz, M., Suciu, A., Barbarino, F., Duca, S., & Lezeu, R. (1976). Protecting action of aspartate on the hepatic changes induced by D-galactosamine. *Arzneimittelforschung, 26*, 855–858.

Froh, M., Zhong, Z., Walbrun, P., Lehnert, M., Netter, S., Wiest, R., et al. (2008). Dietary glycine blunts liver injury after bile duct ligation in rats. *World Journal of Gastroenterology, 14*, 5996–6003.

Goldstein, D. S., Eisenhofer, G., & Kopin, I. J. (2003). Sources and significance of plasma levels of catechols and their metabolites in humans. *Journal of Pharmacology and Experimental Therapeutics, 305*, 800–811.

Grizzi, F., Franceschini, B., Gagliano, N., Moscheni, C., Annoni, G., Vergani, C., et al. (2003). Mast cell density, hepatic stellate cell activation and TGF-beta1 transcripts in the aging Sprague-Dawley rat during early acute liver injury. *Toxicologic Pathology, 31*, 173–178.

Holecek, M., Tilser, I., Skopec, F., & Sprongl, L. (1996). Leucine metabolism in rats with cirrhosis. *Journal of Hepatology, 24*, 209–216.

Lin, Y., SI, D., Zhang, Z., & Liu, C. (2009). An integrated metabonomic method for profiling of metabolic changes in carbon tetrachloride induced rat urine. *Toxicology, 256*, 191–200.

Maillet, E. L., Margolskee, R. F., & Mosinger, B. (2009). Phenoxy herbicides and fibrates potently inhibit the human chemosensory receptor subunit T1R3. *Journal of Medicinal Chemistry, 52*, 6931–6935.

Nowak, A., & Libudzisz, Z. (2006). Influence of phenol, p-cresol and indole on growth and survival of intestinal lactic acid bacteria. *Anaerobe, 12*, 80–84.

Okamoto, T., & Okabe, S. (2000). Carbon tetrachloride treatment induces anorexia independently of hepatitis in rats. *International Journal of Molecular Medicine, 6*, 181–183.

Pan, L., Qiu, Y., Chen, T., Lin, J., Chi, Y., Su, M., et al. (2010). An optimized procedure for metabonomic analysis of rat liver tissue using gas chromatography/time-of-flight mass spectrometry. *Journal of Pharmaceutical and Biomedical Analysis, 52*, 589–596.

Qiu, Y., Su, M., Liu, Y., Chen, M., GU, J., Zhang, J., et al. (2007). Application of ethyl chloroformate derivatization for gas chromatography-mass spectrometry based metabonomic profiling. *Analytica Chimica Acta, 583*, 277–283.

Rechner, A. R., Smith, M. A., Kuhnle, G., Gibson, G. R., Debnam, E. S., Srai, S. K., et al. (2004). Colonic metabolism of dietary polyphenols: influence of structure on microbial fermentation products. *Free Radical Biology and Medicine, 36*, 212–225.

Robertson, D. G., Reily, M. D., Sigler, R. E., Wells, D. F., Paterson, D. A., & Braden, T. K. (2000). Metabonomics: evaluation of nuclear magnetic resonance (NMR) and pattern recognition technology for rapid in vivo screening of liver and kidney toxicants. *Toxicological Sciences, 57*, 326–337.

Sun, J., Schnackenberg, L. K., & Beger, R. D. (2009). Studies of acetaminophen and metabolites in urine and their correlations with toxicity using metabolomics. *Drug Metabolism Letters, 3*, 130–136.

Vulimiri, S. V., Berger, A. & Sonawane, B. (2010). The potential of metabolomic approaches for investigating mode(s) of action of xenobiotics: Case study with carbon tetrachloride. *Mutation Research*, Accession number: 20188855, epub ahead of print.

Wang, X., Su, M., Qiu, Y., NI, Y., Zhao, T., Zhou, M., et al. (2007). Metabolic regulatory network alterations in response to acute cold stress and ginsenoside intervention. *Journal of Proteome Research, 6*, 3449–3455.

Wang, X., Zhao, T., Qiu, Y., Su, M., Jiang, T., Zhou, M., et al. (2009). Metabonomics approach to understanding acute and chronic stress in rat models. *Journal of Proteome Research, 8*, 2511–2518.

Weber, L. W., Boll, M., & Stampfl, A. (2003). Hepatotoxicity and mechanism of action of haloalkanes: Carbon tetrachloride as a toxicological model. *Critical Reviews in Toxicology, 33*, 105–136.

Wiklund, S., Johansson, E., Sjostrom, L., Mellerowicz, E. J., Edlund, U., Shockcor, J. P., et al. (2008). Visualization of GC/TOF-MS-based metabolomics data for identification of biochemically interesting compounds using OPLS class models. *Analytical Chemistry, 80*, 115–122.

Xu, X., Ling, Q., Gao, F., He, Z. L., Xie, H. Y., & Zheng, S. S. (2009). Hepatoprotective effects of marine and kuhuang in liver transplant recipients. *American Journal of Chinese Medicine, 37*, 27–34.

Yuan, H., Ji, W. S., Wu, K. X., Jiao, J. X., Sun, L. H., & Feng, Y. T. (2006). Anti-inflammatory effect of Diammonium Glycyrrhizinate in a rat model of ulcerative colitis. *World Journal of Gastroenterology, 12*, 4578–4581.